Rotating Ring-Disk Electrodes

V. Isomerization and Reductive Coupling of Dialkyl Maleates

Lun-Shu R. Yeh* and Allen J. Bard**

Department of Chemistry, The University of Texas at Austin, Austin, Texas 78712

ABSTRACT

The rates of isomerization and coupling of the radical anions produced on electroreduction of several dialkyl maleates [methyl (DMM), ethyl (DEM), n-butyl (DBM)] in N,N-dimethylformamide solutions were investigated at the rotating ring-disk electrode (RRDE). Digital simulation methods were employed to obtain appropriate working curves and techniques were established to obtain both the first order isomerization constant (k_1) and the second order dimerization constant (k_2) from collection efficiency measurements. The measured k_1 values; DMM, 2.2; DEM, 6.0; and DBM, 6.7 (sec^{-1}) show an increasing isomerization rate with increasing size of alkyl substituent (R). The coupling rates decrease with increasing R; the k_2 values are: DMM, 1.9×10^5; DEM, 9.1×10^4; and DBM, 6.9×10^4 (M^{-1} sec^{-1}). Comparison of these results to previous measurements of the coupling rates of the corresponding trans-species (*i.e.*, fumarates) indicate that the *cis*-radical anions couple about two thousand times faster than do the *trans*.

The rotating ring-disk electrode has been useful in the investigation of the kinetics of electrode reactions, even for rather complicated mechanisms involving parallel reaction paths and higher order reactions [see (1-6) and references therein]. A particularly interesting electrochemical reaction scheme involves the difference in behavior upon reduction of the *cis*- and *trans*-isomeric dialkyl fumarates and dialkyl maleates. Previous

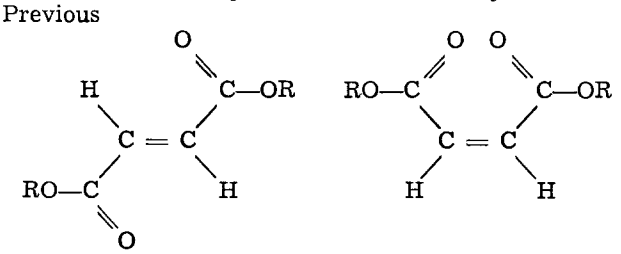

trans-isomer (or F) *cis*-isomer (or M)

R = CH_3 dimethyl fumarate (DMeF)	R = CH_3 dimethyl maleate (DMM)
R = C_2H_5 diethyl fumarate (DEF)	R = C_2H_5 diethyl maleate (DEM)
R = n-C_4H_9 di-n-butyl fumarate (DBF)	R = n-C_4H_9 di-n-butyl (DBM)

studies (7-10) have shown that in aprotic media the fumarates on reduction form the *trans*-radical anion ($F^{-\cdot}$) which undergoes a relatively slow coupling reaction to a dimeric dianion (D^{2-}) which ultimately produces hydrodimer, while the

$$F + e \rightarrow F^{-\cdot} \qquad [1]$$

$$2F^{-\cdot} \rightarrow D^{2-} \qquad [2]$$

maleates form the *cis*-radical anion ($M^{-\cdot}$) which isomerizes to $F^{-\cdot}$ and also couples much more rapidly to produce the dimeric dianion

$$M + e \rightarrow M^{-\cdot} \qquad [3]$$

$$2M^{-\cdot} \xrightarrow{k_2} D^{2-} \qquad [4]$$

$$M^{-\cdot} \xrightarrow{k_1} F^{-\cdot} \qquad [5]$$

While the qualitative nature of the reaction scheme for DEF and DEM was described, the rate constants for the various processes and the effect of alkyl substituent on the rates of isomerization and coupling were not given. The over-all reaction sequence for the reduction of a dialkyl maleate is quite complex and involves, in addition to reactions [2]-[5], the possibility of cross-coupling ([6]) and electron transfer ([7])

$$M^{-\cdot} + F^{-\cdot} \xrightarrow{k_2} D^{2-} \qquad [6]$$

$$M^{-\cdot} + F \xrightarrow{k_2''} F^{-\cdot} + M \qquad [7]$$

We describe here a digital simulation treatment (2-4, 6) of this reaction scheme at the RRDE and a strategy for determination of the rate constants from the experimental data. The values of these constants for the isomerization and coupling rates for several dialkyl fumarates and maleates are reported and discussed.

Experimental

Apparatus.—The general apparatus and procedures have been previously described (5, 8). A Tacussel Electronique Bipotentiostat, Model Bipad 2, was used for all RRDE experiments. A Wavetek function generator provided a linear d-c potential ramp to drive the Bipotentiostat. A simple operational amplifier adder circuit was used to adjust the starting potential of the scan. In all of the experiments, either the disk or ring was held at a constant potential while the other was scanned. The voltammograms were recorded using a Moseley Model 7100B dual pen strip chart recorder. A Moseley Model 2D-2 Autograf X-Y recorder and Model 7005A X-Y recorder were also used to record the disk and the ring currents simultaneously. A Digitec digital voltmeter Model 204 and a Hewlett-Packard digital voltmeter Model IM-102 were used to measure the potentials of the disk and the ring electrodes. These voltmeters were also used to record the steady-state disk and ring currents simultaneously as well as to calibrate the recorder responses. The RRDE, comprising platinum ring and disk electrodes separated by Teflon, was constructed by Pine Instrument Company, Grove City, Pennsylvania, and had the following dimensions: $r_1 = 0.187$ cm, $r_2 = 0.200$ cm, and $r_3 = 0.332$ cm. The theoretical collection efficiency, *i.e.*, the collection efficiency for a stable intermediate generated at the disk electrode, N, for this RRDE is 0.555. The reference electrode was a silver wire, and the counterelec-

* Electrochemical Society Student Member.
** Electrochemical Society Active Member.
Key words: digital simulation, isomerization, dimerization, cyclic voltammetry, reductive coupling.

trode was platinum foil contained in different compartments separated from the main working electrode (RRDE) compartment by medium porosity sintered-glass frits.

Reagents.—N,N-dimethylformamide (DMF) obtained from Matheson, Coleman, and Bell Chemicals, was treated with molecular sieves and anhydrous cupric sulfate and then by vacuum distillation (11). The purified DMF was subjected to at least three freeze-pump-thaw cycles and was then stored in the dry box (Vacuum Atmospheres Corporation, Hawthorne, California). Tetra-n-butylammonium iodide (TBAI), polarographic grade, obtained from Southwestern Analytical Chemicals, Incorporated, was dried under vacuum and stored in the dry box. Diethyl fumarate (DEF), puriss, purchased from Aldrich Chemical Company was used without further purification. Diethyl maleate (DEM) (Matheson, Coleman, and Bell) containing about 5% diethyl fumarate impurity, was stored in a refrigerator. The DEF in the DEM was removed by preparative gas chromatography using a 6 meter chromatographic column filled with 30% SE 30 on 60/80 Chromosorb P and a column temperature of 175°C. Di-n-butyl fumarate (DBF) and di-n-butyl maleate (DBM) were purchased from Aldrich Chemical Company and used as received. Dimethyl maleate (DMM) was prepared by esterification of maleic anhydride with sulfuric acid and methanol purified by vacuum distillation yielding polarographically pure DMM. The maleic anhydride was purchased from Aldrich Chemical Company. The dimethyl fumarate (DMeF), also from Aldrich Chemical Company, was used after sublimation.

Digital simulation.—The RRDE voltammogram for a solution of DEM (2.55 mm) containing a small amount of DEF in 0.1*M* TBAI-DMF is shown in Fig. 1. The disk voltammogram (curve a) which shows the disk current i_d *vs.* disk potential, E_d, is characterized by the reduction of DEF to the radical anion, at −0.75V, (zone II) followed by the reduction of DEM to its radical anion in zone III. Thus for curve a the following reactions occur at the different potentials at the disk electrode surface and in the bulk solution near the electrode:

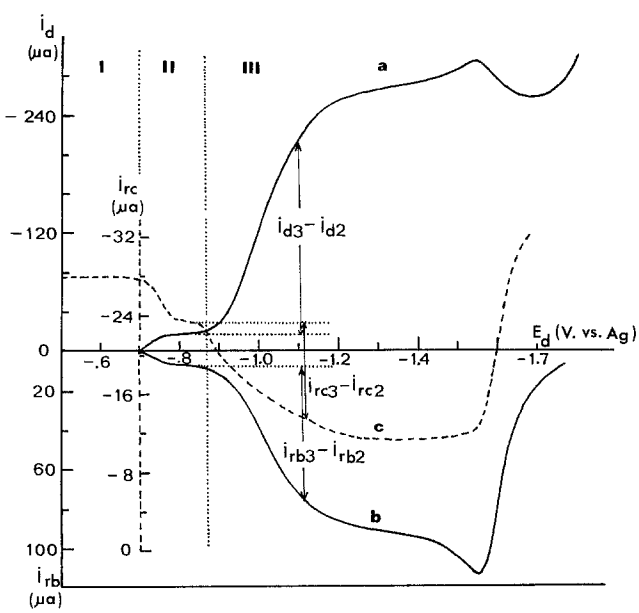

Fig. 1. RRDE voltammograms of diethyl maleate (2.55 mM) with diethyl fumarate impurity in TBAI (0.11M) DMF at a rotation speed of 201 radians/sec. a. Disk current b. Ring current at E_r = 0.0V. c. Ring current at E_r = −0.83V *vs.* Ag R.E.

A. Zone I: no reaction

Zone II: $F + e \rightarrow F^{\cdot -}$ $\quad i_{d2}$

$2F^{\cdot -} \rightarrow D^{2-}$

Zone III: The above reactions and

$M + e \rightarrow M^{\cdot -}$ $\quad (i_{d3} - i_{d2})$

$M^{\cdot -} \rightarrow F^{\cdot -}$ (rotational isomerization)

$2M^{\cdot -} \rightarrow D^{2-}$

$M^{\cdot -} + F^{\cdot -} \rightarrow D^{2-}$

$M^{\cdot -} + F \rightarrow F^{\cdot -} + M$ (charge transfer isomerization)

For the ring electrode held at a ring potential, E_r, of 0.0V any DEF or DEM radical anion formed at the disk which reaches the ring will be oxidized. Thus a scan of the ring current, i_r, *vs.* E_d (curve b) shows waves for the following reactions at the ring in the different zones:

B. Zone I: no reaction

Zone II: $F^{\cdot -} \rightarrow F + e$ $\quad (i_{rb2})$

Zone III: $F^{\cdot -} \rightarrow F + e$ (for $F^{\cdot -}$ generated from F at disk) (i_{rb2})

$F^{\cdot -} \rightarrow F + e$ (for $F^{\cdot -}$ resulting from isomerization) $\}$ $(i_{rb3} - i_{rb2})$

$M^{\cdot -} \rightarrow M + e$

For the ring electrode held at $E_r = -0.83$V (on the reduction plateau for DEF), a plot of i_r *vs.* E_d (curve c) shows waves for the following reactions:

C. Zone I: $F + e \rightarrow F^{\cdot -}$ (reduction of F transported to ring from disk, gap, and directly) (i_{rc1})

Zone II: $F + e \rightarrow F^{\cdot -}$ (shielded reduction of F transported to ring from gap and directly) (i_{rc2})

Zone III: The above reaction and

$M^{\cdot -} \rightarrow M + e$ $\quad (i_{rc3} - i_{rc2})$

The rate constants for the coupling of $F^{\cdot -}$ can be obtained, as previously described, by studies in the absence of maleate. The goal then is to find the rate constants for the isomerization (k_1) and coupling (k_2) of $M^{\cdot -}$ (Eq. [4] and [5]) from the available data. Let us assume first a negligible contribution from the reactions in [6] and [7]. The collection of $M^{\cdot -}$ left after all possible following reactions at the ring is represented by the current $i_{rc3} - i_{rc2}$. Thus the collection efficiency for $M^{\cdot -}$, N_k, is given by

$$N_k = |(i_{rc3} - i_{rc2})/(i_{d3} - i_{d2})| \qquad [8]$$

The ring current which represents the amount of $F^{\cdot -}$

produced by the isomerization of $M^{\cdot -}$ that reaches the ring, I_R, is

$$I_R = (i_{rb3} - i_{rb2}) - (i_{rc3} - i_{rc2}) \quad [9]$$

The total i_r which would be observed for $M^{\cdot -}$ in the absence of any chemical reactions would be $N(i_{d3} - i_{d2})$, where N is the collection efficiency of the electrode. Thus $N(i_{d3} - i_{d2}) - I_R$ is a measure of the extent of the isomerization reaction, and the isomerization collection efficiency parameter, n_k, defined in [10] can be

$$n_k = N - I_R/(i_{d3} - i_{d2}) \quad [10]$$

used to determine k_1. As in earlier work (5-8), a convenient variable is one related to the flux of reduced species from the disk, *i.e.*, $i_{d3} - i_{d2}$, divided by its limiting value (at *ca.* −1.3V), $(i_{d3,l} - i_{d2,l})$ called *CONI*

$$CONI = \frac{i_{d3} - i_{d2}}{i_{d3,l} - i_{d2,l}}$$

The digital simulations were carried out using the programs and methods previously described (2-6), modified for this reaction mechanism. A listing and description is available (12). The following dimensionless parameters were used to represent the rate constants; (notation follows previous practice and the diffusion coefficients of all species were assumed to be equal)

$$XKT = (0.51)^{-2/3}(\nu/D)^{1/3}\omega^{-1}k_1 \quad [11]$$

$$XKTC = (0.51)^{-2/3}(\nu/D)^{1/3}\omega^{-1}Ck_2 \quad [12]$$

Since the isomerization of $M^{\cdot -}$ to $F^{\cdot -}$ is a first order reaction and the half-life of $M^{\cdot -}$ is independent of the original concentration, a straight line parallel to the $1 - CONI$ axis results in the n_k *vs.* $1 - CONI$ plot for $k_1 >> k_2$. On the other hand when $k_2 >> k_1$ the N_k *vs.* $1 - CONI$ plot will show the upward curvature previously reported (6). Because the isomerization does not depend upon concentration or *CONI* when both isomerization and dimerization are significant, the N_k *vs.* $1 - CONI$ curve will generally show the second order dimerization trend, and the effect of isomerization moves the whole curve up or down, depending upon the relative magnitude of the isomerization effect. Simulation results are shown for keeping *XKT* constant and varying *XKTC* (Fig. 2), and keeping *XKTC* constant and varying *XKT* (Fig. 3). Note that when *XKT* predominates, the N_k *vs.* $1 - CONI$ curve straightens out, when *XKTC* does, it is curved. At high *XKT* and low *XKTC* values the line is almost independent of $1 - CONI$. A rough estimate of n_k can be obtained by extrapolating the N_k *vs.* $1 - CONI$ curve to $1 - CONI \rightarrow 1$, where $i_d \rightarrow 0$, and dimerization is negligible compared to isomerization.

The existence of species $F^{\cdot -}$ (either from the presence of more easily reduced F originally in solution or from isomerization of $M^{\cdot -}$) makes consideration of an additional reaction, the cross coupling to form D^{2-}, reaction [6], necessary. Simulations including this possibility were also carried out, with the dimensionless parameter *XKTD* representing the rate of this reaction, where *XKTD* is exactly the same as *XKTC*, except k_2 is replaced by k_2'. These simulations assume that the coupling of two $F^{\cdot -}$'s is slow compared to the $M^{\cdot -}$ reactions, and need not be considered. Typical results are shown in Fig. 4. The results here depend upon the relative amounts of F and M in the bulk solution (taken as 4:1 in the results of Fig. 4) and this provides a method for ascertaining the importance of cross coupling. Increasing the bulk concentration of F decreases the slope of the N_k *vs.* $1 - CONI$ curve.

Similar behavior results from inclusion of the electron transfer cross reaction [7], with *XKTCC* representing the appropriate dimensionless parameter, containing k_2''. The occurrence of this reaction alone, along with isomerization, causes a negative slope in the N_k *vs.* $1 - CONI$ curves (A and B in Fig. 5), as expected from the similar behavior found for the $R + R^{\cdot -}$ reaction in

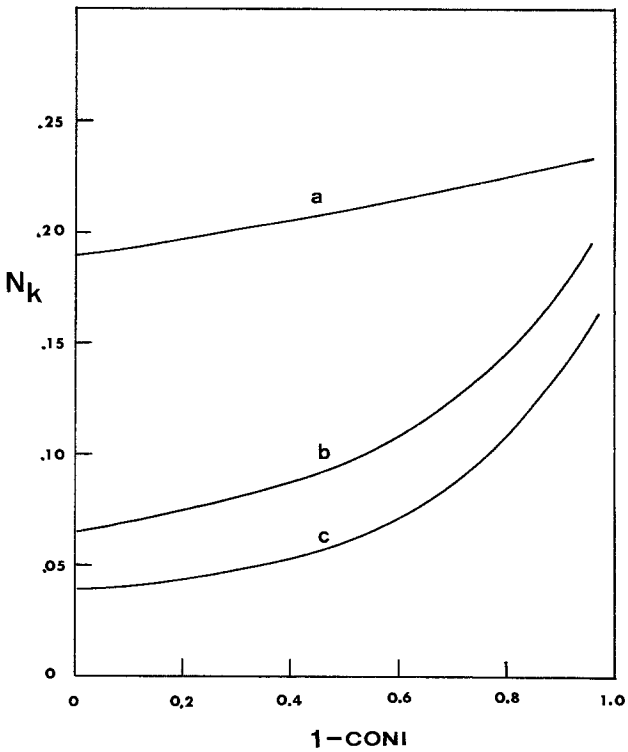

Fig. 2. Simulated collection efficiency for simultaneous reactions: first order parameter *XKT* = 0.77 and second order parameter *XKTC* of a, 0.5; b, 7.0; and c, 15.0.

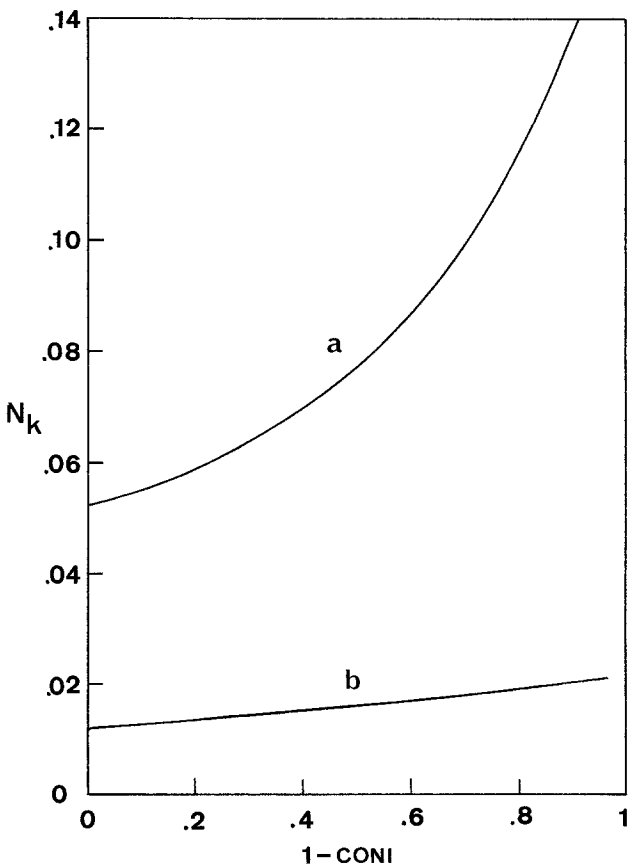

Fig. 3. Simulated collection efficiency for simultaneous reactions: second order parameter *XKTC* = 10, and first order parameter of a, 0.85 and b, 4.0.

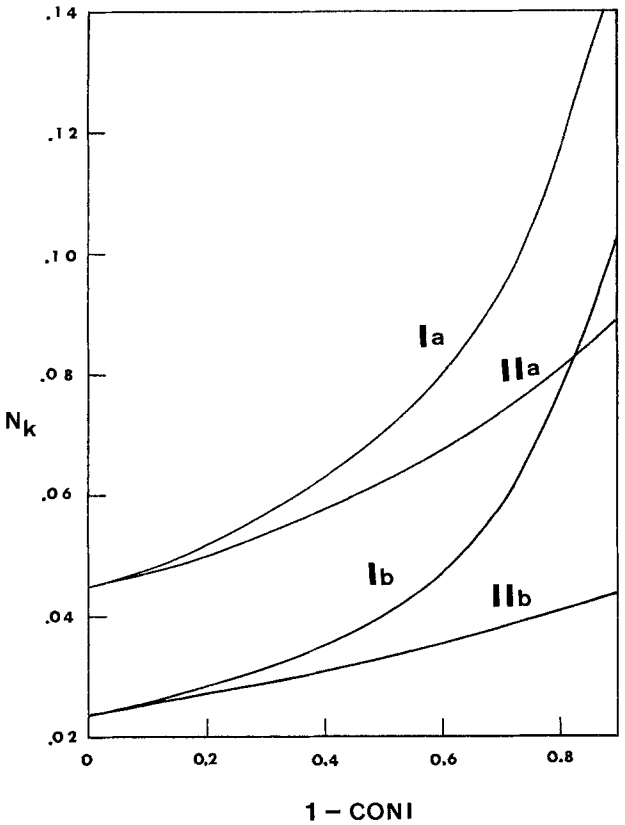

Fig. 4. Collection efficiency for isomerization (*XKT*) and dimerization (*XKTC*) in the presence of cross-coupling dimerization (*XKTD*), [F] = 0.25 [M]). Ia: *XKT* = 0.77, *XKTC* = 13.0; IIa: *XKT* = 0.77, *XKTC* = 7.0, *XKTD* = 7.0; Ib: *XKT* = 0.77, *XKTC* = 30.0; IIb: *XKT* = 0.77, *XKTC* = 15.0, *XKTD* = 15.0.

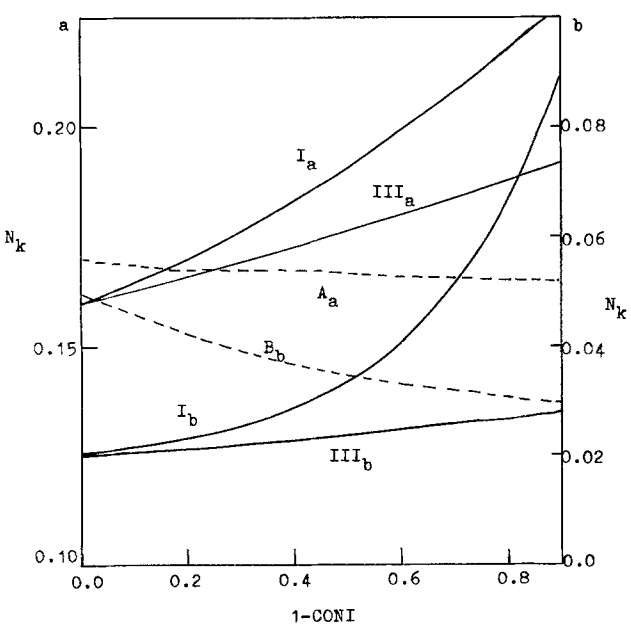

Fig. 5. Collection efficiency for isomerization and dimerization in the presence of $M^{\cdot-}/F$ electron transfer (*XKTCC*). [F] = 0.25 [M]. The subscripts a and b designate the use of a and b scales, respectively. I_a: *XKT* = 0.77, *XKTC* = 0.95; III_a: *XKT* = 0.77, *XKTC* = 0.5, *XKTCC* = 0.25; I_b: *XKT* = 0.77, *XKTC* = 40.0; III_b: *XKT* = 0.77, *XKTC* = 7.0, *XKTCC* = 3.5; A_a: *XKT* = 0.77, *XKTCC* = 0.5; B_b: *XKT* = 0.77, *XKTCC* = 3.5.

hydrodimerizations (6). The inclusion of [7] along with [4] and [5] thus results in decreasing slopes of the working curves (Fig. 5).

Results

Diethyl maleate.—The experimental RRDE voltammogram for DEM containing a small amount of DEF is shown in Fig. 1 and typical experimental results at several values of ω and C are given in Table I. The experimental data were fitted by first obtaining an *XKT* value by simulating the calculated n_k from Eq. [10]. The *XKT* value can also be estimated from the extrapolated N_k value at *CONI* → 0. This value is then used with different trial values of *XKTC*, and the best fit parameters are obtained by a trial and error procedure. The resulting simulated curves based on these two parameters fit the experimental data quite well (Fig. 6). The calculated values of k_1 and k_2 are shown in Table II, based on results with solutions where the DEF concentration was less than 5% that of the DEM. To establish the importance of the cross-coupling reaction [6], experiments where DEF was added to the DEM solutions, were carried out. Typical results of such an experiment, where the concentration of DEF was 24% that of DEM are shown in Fig. 7.

These data could be fitted with a $k_1 = 5.7$ sec^{-1} and $k_2 = 9.6 \times 10^4$ M^{-1} sec^{-1}, which are very close to the values obtained in the absence of excess DEF. This suggests that the $F^{\cdot-}/M^{\cdot-}$ reaction is slow compared to $M^{\cdot-}/M^{\cdot-}$ dimerization. Previous results using double potential step techniques and electron spin resonance spectroscopy (13-15) have fixed the rate constant for the $F^{\cdot-}/F^{\cdot-}$ reaction, [2], under similar conditions at about 44M^{-1} sec^{-1}, so that the *cis*-radical anion dimerizes about 2000 times faster than the *trans*-form.

Dimethyl maleate.—The general behavior of DMM is similar to that of DEM. Freshly prepared DMM, however, does not show a reduction wave for the fumarate during RDE voltammetry, in contrast to the behavior of DEM, where even a sample freshly separated by preparative gas chromatography showed a small DEF wave. A cyclic voltammogram of DMM in the absence of DMeF (Fig. 8) shows an unusual "cross-over" behavior on reversal. On the first reduction scan only the single DMM reduction peak is observed. On the

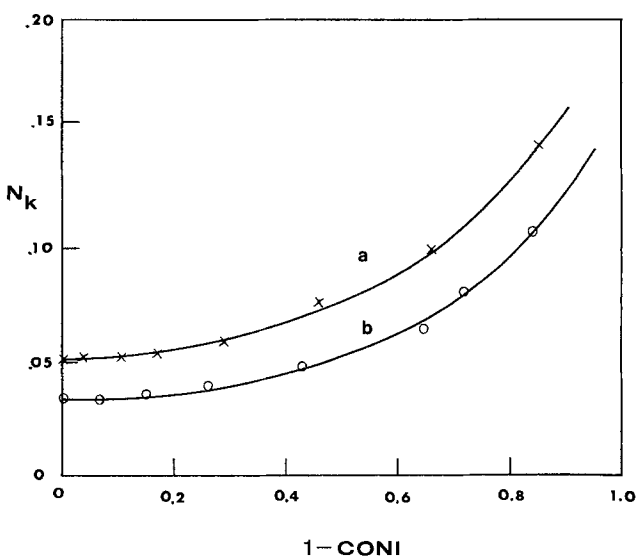

Fig. 6. Collection efficiency of the radical anion of diethyl maleate, 2.65 mM, in 0.1M TBAI-DMF solution, rotation rate at (×) 223 and (○) 164 radians/sec. Solid lines are simulation curves at a, *XKT* = 0.42, *XKTC* = 14.5 (corresponding to k_1 = 6.3 sec^{-1} and $k_2 = 8.25 \times 10^4$ liters/mole-sec); b, *XKT* = 0.53, *XKTC* = 24.0 (corresponding to $k_1 = 5.9$ sec^{-1} and $k_2 = 10.0 \times 10^4$ liters/mole-sec).

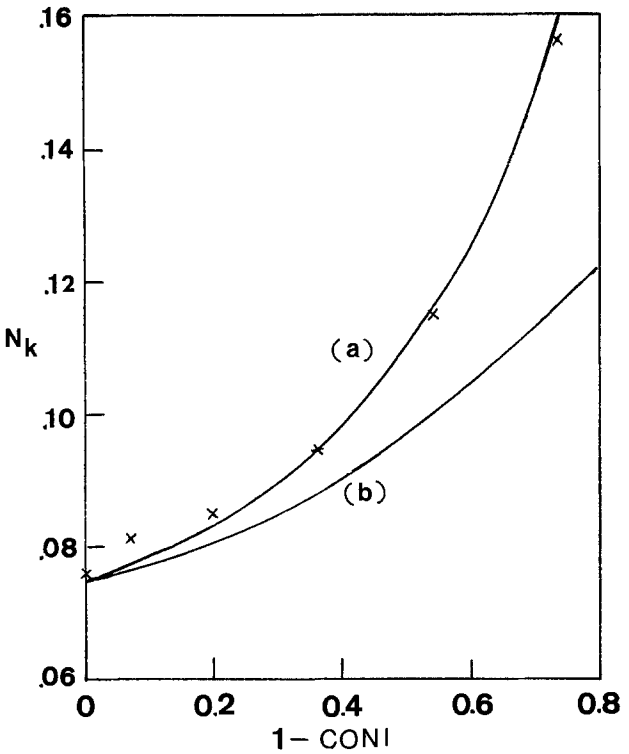

Fig. 7. Collection efficiency of the radical anion of diethyl maleate, 0.95 mM, in the presence of diethyl fumarate, 0.23 mM, in 0.1M TBAI-DMF solution. Experimental results (x) were obtained at rotation rate of 164 radians/sec. Solid lines are simulation curves at (a), $XKT = 0.51$, $XKTC = 7.0$ (corresponding to $k_1 = 5.7$ sec^{-1} and $k_2 = 9.6 \times 10^4$ liters/mole-sec); (b), $XKT = 0.51$, $XKTC = 4.5$, $XKTD = 4.5$.

reverse scan (oxidation of $M^{\cdot-}$ and $F^{\cdot-}$) the curve crosses over the reduction scan curve. This effect implies that a greater amount of reduction in this region (at *ca.* −0.9V) is occurring on the reverse scan than on the forward one. This can be attributed to the $M^{\cdot-}$ catalyzed isomerization of M to F (7) via the reaction sequence [3], [5], and [7], so that the amount of F at the electrode surface on reversal is larger than that present during the first forward scan. Note that this behavior does not occur with subsequent scans or for solutions originally containing DMeF. Similar cyclic voltammograms have been noted by Saveant (16). Notice also that the M reduction wave decreases strongly on repeated scans because of the loss of M via the dimerization, while the $F/F^{\cdot-}$ couple establishes a steady-state wave pair. RRDE studies of DMM exactly parallel those of DEM; typical data are in Table I and the resulting values of k_1 and k_2 are listed in Table II. Experiments in which DMeF was added in amounts up to 25% that of DMM were carried out and again the cross-coupling reaction did not appear to affect the results to a significant extent. Previous measurements of the dimerization rate of DMeF radical anion (5, 14) yield a rate constant of *ca.* $110M^{-1}$ sec^{-1} again about 2000 times smaller than that of the *cis*-radical anion.

Di-n-butyl maleate.—The behavior of DBM is very similar to that of DEM; both show the presence of the fumarate even in highly purified samples. The RRDE experiments parallel those of DEM; typical data and results are given in Tables I and II. The rate constant for DBF radical anion dimerization has been reported as $25M^{-1}$ sec^{-1} (14).

Discussion

The effect of substituent (methyl, ethyl, n-butyl) for the maleates is opposite for the isomerization (k_1) and dimerization (k_2) rate constants. For the dimerization, as the size of the substituent is increased, k_2 decreases; a similar trend is observed for the fumarates (14). Thus the bulky groups hinder the coupling of the radical anions, as expected. For the isomerization, increasing the substituent size causes k_1 to increase. The radical anions isomerize much more rapidly than the parent compounds probably because (*i*) the addition of an electron to the antibonding molecular orbital causes a decrease in the bond order of the central ethylenic bond and (*ii*), the negative charge on the molecule resides to a large extent on the oxygens, causing a coulombic repulsion of the carbonyl groups. Increasing the size of the substituents provides an added steric repulsion and thus increases k_1. Finally, for all compounds the *cis*-radical anions dimerize about 2000 times as rapidly as the *trans*. This can be explained by a larger electron density residing on the ethylenic carbons because of the coulombic repulsion of charge from the *cis*-carbonyls or because of partial twisting around the central bond. Not only is the coupling reaction larger, but these *cis*-radical anions react more rapidly with

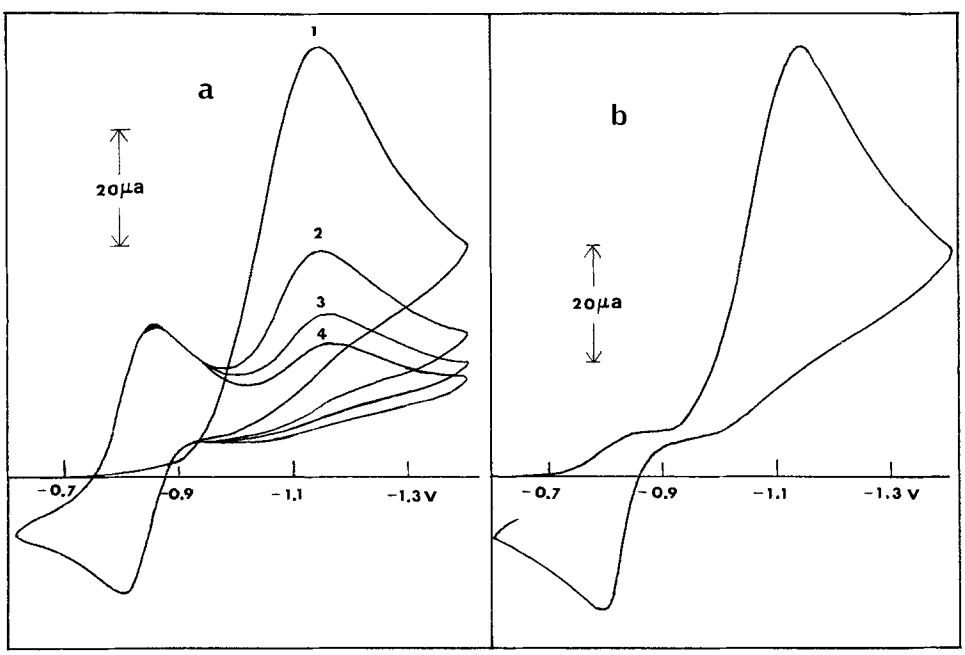

Fig. 8. Cyclic voltammograms of 2.0 mM dimethyl maleate in 0.1M TBAI-DMF solution, voltage scan rate was at 200 mV/sec; a, polarographically pure dimethyl maleate with continuous scans; and b, in the presence of dimethyl fumarate as impurity.

Table I. RRDE results for dialkyl maleates in 0.1M TBAI-DMF solution

ω (sec^{-1})	$i_{d3}-i_{d2}$ ($-\mu a$) (A)	$i_{rb3}-i_{rb2}$ (μa) (B)	$i_{rc3}-i_{rc2}$ (μa) (C)	$N_k=\frac{(C)}{(A)}$	$N-\frac{n_k=}{(B)-(C)}{(A)}$	CONI
			A. Diethyl maleate			
			(a) 1.85 mM			
164	13.5	5.35	2.09	0.155	0.314	0.108
	27.5	10.06	3.44	0.125	0.313	0.220
	46.5	15.35	4.25	0.0914	0.316	0.372
	59.0	18.60	4.75	0.0805	0.320	0.472
	72.0	22.20	5.15	0.0715	0.317	0.576
	92.0	27.90	5.80	0.0630	0.315	0.736
	112.0	33.30	6.30	0.0562	0.314	0.892
	125.0	36.80	6.60	0.0528	0.313	1.000
223	27.5	10.25	4.54	0.165	0.347	0.187
	45.5	15.6	5.92	0.130	0.341	0.310
	67.0	21.6	7.25	0.108	0.340	0.456
	87.0	26.2	7.70	0.0885	0.342	0 592
	110	31.6	8.70	0.079	0.347	0.748
	131	36.4	9.55	0.073	0.350	0.891
	147	40.4	9.85	0.067	0.347	1.000
			(b) 2.65 mM			
164	34.7	12.2	3.7	0.107	0.310	0.164
	59.7	19.6	4.78	0.080	0.306	0.283
	77.0	23.8	5.0	0.065	0.311	0.365
	120.0	35.5	5.8	0.048	0.307	0.569
	155	45.5	6.05	0.039	0.301	0.734
	180	52 2	6.4	0.0355	0.301	0.853
	195	55.6	6.8	0.035	0.305	0.924
	211	59.8	7.2	0.034	0.306	1.000
223	36.5	13.3	5.3	0.145	0.336	0.150
	82.0	25.7	8.05	0.098	0.339	0.337
	131	37.9	10.0	0.076	0.341	0.539
	172	46.4	10.3	0.060	0.345	0.708
	201	53.6	10.8	0.054	0.342	0.827
	221	59.0	11.6	0.052	0.340	0.909
	234	62.5	12.2	0.052	0.339	0.963
	243	64.9	12.6	0.052	0.340	1.000
			B. Dimethyl maleate			
			(a) 0.52 mM			
106	8.9	2.46	0.99	0.111	0.390	0.299
	13.6	3.55	1.20	0.088	0.382	0.456
	18.5	4.53	1.38	0.075	0.385	0.621
	24.5	5.60	1.49	0.061	0.388	0.822
	28.2	6.45	1.60	0.057	0.383	0.946
	29.8	6.92	1.70	0.057	0.380	1.00
164	13.2	3.47	1.75	0.132	0.425	0.353
	18.8	4.53	2.03	0.108	0.422	0.503
	26.7	5.55	2 21	0.083	0.430	0.714
	31.5	6.46	2.40	0.076	0.426	0.842
	37.4	7.57	2.67	0.071	0.424	1.00
			(b) 1.05 mM			
106	10.8	2.98	1.30	0.120	0.399	0.174
	21.4	4.72	1.50	0.070	0.405	0.346
	30.3	6.27	1.82	0.060	0.408	0.489
	39.4	7.76	1.96	0.050	0.408	0.636
	49.5	9.50	2.19	0.044	0.407	0.800
	55.5	10.56	2.36	0.042	0.407	0.897
	61.9	11.90	2.56	0.041	0.404	1.00
164	24.4	5.62	2.58	0.106	0.430	0.323
	34.8	7.10	2.85	0.082	0.435	0.461
	45.2	8.72	3.21	0.071	0.433	0.600
	58.0	10.22	3.55	0.061	0.440	0.768
	65.5	12.00	3.76	0.057	0.429	0.867
	75.5	13.90	4 29	0.057	0.428	1.00
			C. Di-n-butyl maleate			
			1.30 mM			
180	12.8	5.5	2.24	0.175	0.300	0.144
	22.5	9.0	3.37	0.150	0.305	0.253
	38.1	14.0	4.38	0.115	0.302	0.428
	53.7	18.4	5.13	0.096	0.309	0.604
	67.5	22.0	5.26	0.078	0.307	0.870
	83.5	27.2	6.26	0.075	0.304	0.940
	89.0	28.7	6.38	0.072	0.304	1.000
230	17.1	7.4	3.6	0.210	0.333	0.143
	25.0	10.1	4.5	0.180	0.330	0.242
	42.4	15.7	6.3	0.148	0.333	0.410
	60.6	21.4	7.5	0.124	0.327	0.590
	76.9	25.6	8.1	0.105	0.328	0.745
	96.2	30.6	9.1	0.094	0.331	0.933
	103.0	32.5	9.5	0.092	0.331	1.000

added electrophiles such as acrylonitrile (7) or CO_2 (12, 17).

We conclude by referring to some related studies of isomerization of radical anions. Hayon and Simic (18) used a pulse radiolysis technique to study the formation and reactions of DMM and DMeF radical anions in aqueous solutions. They found no appreciable isomerization of $DMM^{\cdot-}$ within the time window of their experiment ($\sim$ 0.1 μsec), which is consistent with the k_1 value reported here. Moreover strong hydrogen bonding in water may stabilize the *cis*-configuration. Ion pairing can also stabilize the radical anion and decrease the isomerization rate. Thus Szwarc and co-workers (19, 20) found that in THF solutions in the presence of alkali metal ions, stilbene radical anion isomerized slowly and the over-all isomerization reaction proceeded via the ion paired dianion. In HMPA, however, where the ion pairs were dissociated, isomerization of *cis*-stilbenide was reported. A study of the effect of ion pairing on the isomerizaton of maleate radical anions in DMF would be of interest but would probably be difficult, because the dimerization rates would be expected to become very rapid under these conditions (14).

Table II. Calculated isomerization rate constant (k_1) and dimerization rate constant (k_2) of dialkyl maleate radical anions from RRDE results in 0.1M TBAI-DMF solutions

Conc (mM)	ω (sec^{-1})	XKT	k_1 (sec^{-1})	XKTC	k_2 (M^{-1} sec^{-1})
			A. Diethyl maleate		
1.85	164	0.5	5.6	13.0	9.12×10^4
	223	0.41	6.2	9.5	9.06
2.65	164	0.53	5.9	24.0	10.0
	223	0.42	6.3	14.5	8.25
			Avg.: 6.0		9.1×10^4
			B. Dimethyl maleate		
0.52	106	0.30	2.15	13.0	1.75×10^5
	164	0.22	2.44	10.5	2.24
1.05	106	0.26	1.86	25.5	1.74
	164	0.21	2.33	16.5	1.75
			Avg.: 2.20		1.9×10^5
			C. Di-n-butyl maleate		
1.30	180	0.53	6.4	7.7	7.20×10^4
	230	0.45	7.0	5.5	6.57
			Avg.: 6.7		6.9×10^4

Acknowledgment

The support of this research by the Robert A. Welch Foundation and the National Science Foundation (CHE 71-03344) is gratefully acknowledged.

Manuscript submitted July 7, 1976; revised manuscript received Sept. 24, 1976.

Any discussion of this paper will appear in a Discussion Section to be published in the December 1977 JOURNAL. All discussions for the December 1977 Discussion Section should be submitted by Aug. 1, 1977.

Publication costs of this article were assisted by The University of Texas.

REFERENCES

1. W. J. Albery and M. L. Hitchman, "Ring-Disc Electrodes," Oxford University Press, London (1971).
2. K. B. Prater and A. J. Bard, *This Journal*, **117**, 207 (1970).
3. *Ibid.*,335 (1970).
4. *Ibid.*, 1517 (1970).
5. V. J. Puglisi and A. J. Bard, *ibid.*, **119**, 829 (1972).
6. *Ibid.*, **119**, 833 (1972).
7. A. J. Bard, V. J. Puglisi, J. V. Kenkel, and A. Lomax, *Faraday Discuss. Chem. Soc.*, **56**, 353 (1973).
8. V. J. Puglisi and A. J. Bard, *This Journal*, **120**, 748 (1973).
9. A. V. Il'yasov, Yu. M. Kargin, and V. Z. Kondranina, *Izv. Akad. Nauk. SSR, Ser Khim.*, **5**, 927 (1971).
10. A. V. Il'yasov, Yu. M. Kargin, N. N. Sotnikova, V. Z. Kondranina, B. V. Mel'nikov, and A. A. Vafina, *ibid.*, **5**, 932 (1971).
11. L. R. Faulkner and A. J. Bard, *J. Am. Chem. Soc.*, **90**, 6284 (1968).
12. L. S. R. Yeh, Ph.D. Dissertation, The University of Texas at Austin, Austin, Texas (1976).
13. W. V. Childs, J. T. Maloy, C. P. Keszthelyi, and A. J. Bard, *This Journal*, **118**, 874 (1971).
14. M. J. Hazelrigg and A. J. Bard, *ibid.*, **122**, 211 (1975).
15. I. B. Goldberg, D. Boyd, R. Hirasawa, and A. J. Bard, *J. Phys. Chem.*, **78**, 295 (1974).
16. J. M. Saveant, Private communication (1976).

17. L. S. R. Yeh and A. J. Bard, *This Journal*, To be published.
18. E. Hayon and M. Simic, *J. Am. Chem. Soc.*, **95**, 2433 (1973).
19. G. Levin, T. A. Ward, and M. Szwarc, *ibid.*, **96**, 270 (1974).
20. T. A. Ward, G. Levin, and M. Szwarc, *ibid.*, **97**, 258 (1975).

Electrochemical Studies of Antitumor Antibiotics

I. Cyclic Voltammetric Study of Mitomycin B

Gopalakrishna M. Rao,* J. William Lown, and James A. Plambeck*

Department of Chemistry, University of Alberta, Edmonton, Alberta, Canada

ABSTRACT

Mitomycin B, a mitosane quinone-containing antibiotic, was investigated by HMDE cyclic voltammetry in aqueous media at 37.5°C. The observations are consistent with a mechanism in which mitomycin B is reversibly reduced, at −0.200V *vs.* SCE, to the hydroquinone, following which the aziridine ring opens rapidly. The significance of the mechanism is discussed in relation to the antineoplastic activity of certain antibiotics of the mitosane class.

Mitomycin B, **1**, is a member of the mitosane class of agents and is produced by *Streptomyces caespitosus* together with mitomycin C, an antitumor antibiotic of clinical significance (1, 2). This class of agents is part of the larger group of aminoquinone-containing antibiotics which act as inhibitors of DNA synthesis, such as streptonigrin (3), porfiromycin (1), the actinomycins (4), and aziridinoquinones (5), many of which exhibit significant antineoplastic activity. It is currently considered (6) that the mitosanes *in vivo* undergo an initial reduction by a cellular reductase, mediated by NADPH, to form the hydroquinones. The latter rapidly lose methanol or water to form an activated species which can induce covalent cross-links between complementary strands of DNA. These cross-links prevent strand separation during the semiconservative replication process (2)

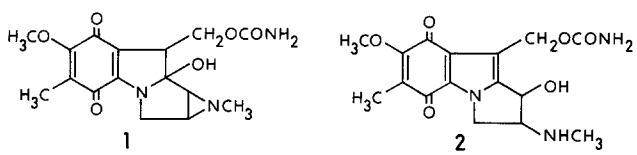

Mitomycin C and related quinone-containing derivatives have been observed to cause extensive degradation of DNA in addition to cross-linking (7, 8). Hitherto this has been attributed to the stimulation of the production of intracellular deoxyribonucleases in the cell repair cycle (9, 10). Recently, however, we demonstrated (11) that when mitomycin C and streptonigrin are reduced in the presence of oxygen they generate superoxide and hydroxyl radicals which degrade DNA by single strand scission analogous to radiation damage.

For these reasons a detailed study of the redox behavior of the mitosanes is of interest; it is our purpose to investigate the initial reduction process *in vitro*, together with such related chemical processes as are accessible to electroanalytical investigation.

Experimental

The Princeton Applied Research (PAR) Model 9300-9301 polarographic cell was employed in a three-electrode configuration which included a conventional aqueous saturated calomel reference electrode, to which all potentials in this paper are relative unless otherwise specified, a platinum counterelectrode, and a PAR Model 9323 hanging mercury drop working electrode. The cell temperature was maintained at physiological temperature of 37.5° ± 0.02°C by circulation of thermostated water. Cyclic voltammetry was done using the PAR Model 173-175-176 configuration. The resulting curves were recorded on an X-Y recorder or photographed on an oscilloscope as required by the scan rate, ν, which was varied from 20 mV/sec to 500 V/sec. The pH of each solution was measured both before and after each run using an Accumet Model 520 pH meter and a combination glass-SCE electrode.

Samples of mitomycin B were kindly supplied by American Cyanamid Company Lederle Laboratories, Pearl River, New York, and by Kyowa Hakko Chemical Company, Japan, and were used as received. A derivative of this compound, **2**, in which the aziridine ring was opened was prepared by mild acid hydrolysis according to the procedure of Stevens *et al.* (12). The crude hydrolysate was then recrystallized from the mixture of ether and pentane as a yellow-orange solid. This derivative **2**, which we do not believe to have been prepared previously, is a yellow solid, mp 70°-72°C, soluble in water, chloroform, and ether; it can be precipitated from ether by addition of pentane. Its spectral characteristic absorbances (nanometers) and log of molar absorptivity are: 236, 4.16; 286, 4.06; 355, 3.26; 442, 2.89. Its infrared spectrum in $CHCl_3$ has the following absorbances (nanometers): 2960, 2920 (CH_3 sym. str.); 2860; 1715 (carbamate C=O); 1660, 1645 (quinone C=O); 1595; 1450; 1395; 1250 (=C—O—C antisym. str.); 1085; 1000 (=C—O—C sym. str.). All other chemicals were reagent grade and were used without further purification.

Fresh stock solutions of $1.3 \times 10^{-3}M$ mitomycin B were prepared daily and protected from light. Sample solutions were prepared in a cell itself as $3.3 \times 10^{-4}M$ mitomycin B, 0.1*M* phosphate buffer, and 0.1*M* KCl supporting electrolyte. The derivative **2** was treated in a similar manner. All solutions were deaerated with purified nitrogen for 10 min prior to a run and blanketed with it during a run.

Results

Typical results for the cyclic voltammetry of **1** at pH 6.58 are shown in Fig. 1, which shows a pair of well-defined peaks (cathodic IC and anodic IA) and a second pair of small peaks (cathodic IIC and anodic IIA). No other peaks were observed even when the potential scan was extended up to supporting electrolyte discharge at −1.6V.

* Electrochemical Society Active Member.
Key words: cyclic voltammetry, antibiotic mitosane, quinone, DNA, antineoplastic, antitumor.